THE JOURNAL OF BIOLOGICAL CHEMISTRY VOL. 287, NO. 8, pp. 5639–5649, February 17, 2012

DNA Methylation-regulated miR-193a-3p Dictates Resistance of Hepatocellular Carcinoma to 5-Fluorouracil via Repression of SRSF2 Expression*[S]

Received for publication, August 8, 2011, and in revised form, November 12, 2011 Published, JBC Papers in Press, November 23, 2011, DOI 10.1074/jbc.M111.291229

Kelong Ma[‡§1], Yinghua He[§1], Hongyu Zhang[§1], Qi Fei[§], Dandan Niu[§], Dongmei Wang[¶], Xia Ding[¶], Hua Xu[‖], Xiaoping Chen[‖], and Jingde Zhu[§2]**

*From the [‡]Shanghai Medical College, Fudan University, Shanghai 200032, China, the [§]Cancer Epigenetics Program, Shanghai Cancer Institute, Renji Hospital, Shanghai Jiaotong University, Shanghai 200032, China, the [¶]Anhui Key Laboratory of Cellular Dynamics and Chemical Biology, University of Science and Technology of China, Hefei 230027, China, the [‖]Department of Liver Surgery, Tongji Hospital, Huazhong University of Science and Technology of China, Wuhan 430074, China, and the **Center for Basic and Translational Epigenetic Research of Diseases, School of Life Science, Anhui Medical University, Hefei 230032, China*

Background: Chemoresistance prevents effective therapy of hepatocellular carcinoma (HCC).
Results: Genomic and mechanistic studies suggested the role of miR-193a-3p via SRSF2 mediates up-regulation of the proapoptotic splicing form of caspase 2 in HCC 5-FU resistance.
Conclusion: We identify a novel molecular mechanism underlying 5-FU resistance in HCC.
Significance: These molecular events identified provide a set of prognostic markers for future rational 5-FU therapy in HCC.

Chemoresistance prevents effective cancer therapy and is rarely predictable prior to treatment, particularly for hepatocellular carcinoma (HCC). Following the chemoresistance profiling of eight HCC cell lines to each of nine chemotherapeutics, two cell lines (QGY-7703 as a sensitive and SMMC-7721 as a resistant cell line to 5-fluorouracil (5-FU) treatment) were systematically studied for mechanistic insights underpinning HCC 5-FU chemoresistance. Genomic profiling at both DNA methylation and microRNA (miR) levels and subsequent mechanistic studies illustrate a new mechanism for how DNA methylation-regulated miR-193a-3p dictates the 5-FU resistance of HCC cells via repression of serine/arginine-rich splicing factor 2 (SRSF2) expression. In turn, SRSF2 preferentially up-regulates the proapoptotic splicing form of caspase 2 (CASP2L) and sensitizes HCC cells to 5-FU. Forced changes of miR-193a-3p level reverse all of the phenotypic features examined, including cell proliferation, cell cycle progression, and 5-FU sensitivity, in cell culture and in nude mice. Importantly, the siRNA-mediated repression of SRSF2 phenocopies all of the miR-193a-3p mimic-triggered changes in QGY-7703. This newly identified miR-193a-3p-SRSF2 axis highlights a new set of companion diagnostics required for optimal 5-FU therapy of HCC, which involve assaying both the DNA methylation state of the miR-193a gene and the expression of miR-193a-3p and SRSF2 and the relative level of the proapoptotic *versus* antiapoptotic splicing forms of caspase 2 in clinical samples.

Cancer is a complex disease with extensive genetic and epigenetic defects; the archives of both are rapidly updated by the second generation sequencing-based genome-wide analyses at the DNA sequence (1), DNA methylation state (2), and protein and RNA levels (3). Among the epigenetic entities, which refer to the DNA sequence-independent mechanisms underlying the cross-cell generational transmission of gene expression memory, DNA methylation (the addition of the methyl group at the cytosine ring of the 5′-CpG-3′ sequence) is the best characterized and is regarded as a promising molecular indicator for the existence and/or prognostic state of cancer (4, 5). Micro-RNAs (miRs)[3] are small noncoding RNAs that regulate the expression of the protein-coding genes, including the genes controlling the DNA methylation state of the genome (6), at both RNA stability and translational levels in a sequencing-specific manner. The DNA methylation state of the promoter region of a subset of miR genes negatively correlates with their transcription state (7–9). Aberrant miR expression has also been regarded as a promising biomarker for cancer detection (10, 11).

Hepatocellular carcinoma (HCC) is one of the most aggressive and common malignancies, ranking second highest in terms of cancer mortality rate worldwide and in mainland China (12) (see the World Health Organization GLOBOCAN Web site). Surgical removal of tumors followed by systemic chemotherapy is a preferred treatment for patients with localized disease (13, 14). Patients with advanced disease are routinely treated by transarterial chemoembolization and systemic

* This work is supported by National Science Foundation Grant 30921140312 (to J. Z.), National Research Program for Basic Research Grants 2009CB825606, 2009CB825607, and 2010CB912802 (to J. Z.), and International Collaboration Grant 2009DFA31010 (to X. D.). This work was also supported by China National Key Projects for Infectious Disease Grant 2008ZX10002-021 (to D. W.), and Shanghai Science Foundation Grant 09JC141300.

[S] This article contains supplemental Figs. S1–S3.

[1] These authors contributed equally to this work.

[2] To whom correspondence should be addressed: Cancer Epigenetics Program, Shanghai Cancer Institute, Renji Hospital, Shanghai Jiaotong University, Shanghai 200032, China. Tel.: 8621-64224285; Fax: 8621-64224285; E-mail: jdzhu@sjtu.edu.cn.

[3] The abbreviations used are: miR, microRNA; HCC, hepatocellular carcinoma; 5-FU, 5-fluorouracil; MTT, 3-(4,5-dimethylthiazol-2-yl)-2,5-diphenyltetrazolium bromide; qRT-PCR, quantitative RT-PCR; MSP, methylation-specific PCR; BSP, bisulfite sequencing PCR.

chemotherapy using doxorubicin, cisplatin, interferon, or 5-fluorouracil (5-FU), despite the uncertain clinical benefits (14, 15). New molecular agents and antibodies targeting the defective signaling pathways have also been attempted for treating HCC, so far with limited success (14, 16). Therefore, there is a compelling need for a robust diagnostics for early detection and (stratification) staging of the disease to maximize clinical benefits and minimize the toxicity and cost of nonsurgical treatments. For better mechanistic understanding of the chemoresistance of HCC cancer, we carried out a chemoresistance profiling of eight HCC cell lines to each of nine conventional chemotherapeutics and performed both genome-wide analysis and mechanistic studies of a pair of HCC cell lines that differ drastically in chemoresistance to 5-FU but to none of the rest drugs analyzed. The systematic studies targeting a DNA methylation-regulated miR-193a-3p as the first candidate of several dozen informative defects were studied in detail for both its role in HCC 5-FU resistance and the mechanistic details in both cell culture and a tumor xenograft nude mouse model.

EXPERIMENTAL PROCEDURES

Analysis at Cellular Level

Human HCC cell lines were as follows: QGY-7703 (Cell Bank (Shanghai, China), no. TCHu43) (17), SMMC-7721 (Cell Bank, no. TCHu52), BEL-7402 (Cell Bank, no. TCHu10), HepG2 (ATCC (Manassas, VA), no. HB-8065), Hep3B (ATCC, no. HB-8064), PLC (ATCC, no. CRL-8024), YY-8103, and FOCUS (18). The log phase of cell culture was obtained in Dulbecco's modified Eagle's medium (1:1; Invitrogen) containing 10% calf serum and 1% streptomycin-penicillin at 37 °C in 5% CO_2.

The thiazolyl blue tetrazolium blue (MTT)-based cell proliferation assay was carried out as follows. 5×10^3 to 1×10^4 cells in triplicate were cultured into each well of a 96-well plate (in triplicate) for 72 h, followed by a 3-h 37 °C incubation after the addition of 10 μl (5 mg/ml) of MTT salt (Sigma). The $A_{570\ nm}$ reading was obtained, and the mean and S.D. of the triplicate experiments were calculated and plotted (19). To determine the IC_{50}, cells in triplicate were subjected to a series dilution of each drug for 72 h, followed the MTT-based analysis. The relative $A_{570\ nm}$ readings (mean and S.D.) in each drug-treated set and in the no-drug mock sample were calculated (percentage) and plotted against the logarithm of the drug concentration. The linear regression parameters were determined for each curve, and the IC_{50} value was extrapolated (20). Sources of the drugs are as follows: 5-FU, Shanghai Xudong Haipu Pharmaceutical (Shanghai, China); gemcitabine, Jiangsu Hansen Pharmaceutical (Lianyungang, China; epirubicin, Shenzhen Main Luck Pharmaceutical (Shenzhen, China); irinotecan, Aventis Pharmaceutical (Frankfurt, Germany); paclitaxel, Bristol-Myers Squibb Co.; mitomycin, Hisun Pharmaceutical (Taizhou Zhejiang, China); docetaxel, Jiangsu Hengrui Medicine (Lianyungang, China); vinorelbine, Yangzhou Aosaikang Pharmaceutical (Jiangsu, China); and cisplatin, Qilu Pharmaceutical Factory (Jinan, China).

Luciferase Reporter Assay

The seed sequences (miR-193a-3p, 5′-AATT TGGGTCTTTGCGGGCGAGATGAT-3′ and 5′-CTAGATCATCTCGCCCGCAAAGACCCA-3′; miR-127–3p, 5′-AATTCTGAAGCTCAGAGGGCTCTGATT-3′ and 5′-CTAGAATCAGAGCCCTCTGAGCTTCAG-3′) were annealed and inserted into the EcoRI and XbaI sites of the CMV promoter-driven firefly luciferase reporter, pCDNA3.1-luc, to make miR-193a-3p-luc and pGL3-miR-127–3p-luc (as an unrelated control) luciferase reporter constructs, respectively. The analysis mediated with Lipofectamine™ 2000 (Invitrogen) transfection/reporter was performed as described previously (21). The cells at 60% confluence were transfected in duplication by 25 ng luciferase reporter, 50 ng carrier plasmid DNA together with 5 ng of CMV-Renilla luciferase (to control transfection efficacy) luciferase activities of the transfected cells were measured after 24 h with a dual luciferase reporter system (Promega, Madison, WI) by MiniLumat LB 9506 (Berthold, Germany). The S.D. of the ratio of the firefly luciferase over the *Renilla* luciferase activity of the duplicates was plotted against the tested constructs. All of the experiments were carried out at least three times, and the result from one representative experiment was presented (21). The miR-193a-3p mimic and antagomir (Ribobio, Guangzhou, China) transfection was performed at dose of 10 and 50 nM, respectively.

For the cell cycle profiling, cells were seeded in 6-well plates at 40% confluence and incubated at 37 °C for 24 h before transfection with the mock (non-related mimic or antagomir), miR-193a-3p mimic, or antagomir with miR-193a-3p-luc reporter/CMV-*Renilla* reporter constructs. The transfected cells were collected and fixed by 70% ethanol at −20 °C for 24 h, stained with 50 μg/ml propidium iodide (Sigma), and analyzed on a fluorescence-activated cell sorter (FACS) according to the manufacturer's instructions (BD Biosciences). All flow cytometry experiments were performed at least three times, and a representative experiment is shown.

Analysis at Molecular Level

Protein—Cells were lysed by the 1× SDS loading buffer (60 mM Tris-HCl, pH 6.8, 2% SDS, 20% glycerol, 0.25% bromphenol blue, 1.25% 2-mercaptoethanol) and then sonicated to shear the genomic DNA (Bioruptor, Diagenode, Belgium)/Western blot-analyzed with antibodies: anti-SRSF2 (AP2800a), anti-E2F1 (AP7593a), anti-E2F6 (AP6637c), anti-YWHAZ (AP8152c), anti-HDAC1(AP1101a), anti-MCL1 (AP1312a), anti-PCNA-(AP2835b), anti-PHF8 (AP9276b), anti-thymidylate synthetase (AP6682b), anti-PTK2 (AP8614b), anti-CDC5L (AP8949c) (Abgent, San Diego, CA), and anti-β-actin (Sigma), respectively. The target proteins were then probed with anti-rabbit IgG peroxidase-conjugated antibody (KangChen Bio-tec, Shanghai, China), followed by an enhanced chemiluminescence reaction (Pierce). The relative levels of proteins were quantified by densitometry with the FR-200A Analysis System (Fu-Ri Technology, Shanghai, China).

RNA—Total RNA was isolated using TRIzol reagent (Invitrogen). Complementary DNA synthesis was performed using a primeScript RT reagent kit (Tiangen Biotech Co., Ltd., Beijing, China) for the SYBR Green-based real-time PCR analysis in the

Rotor-Gene™ 6000 system (Qiagen) of SRSF2, E2F1, ABCC8, and CASP2S/L. The expression of miR-193a-3p (Ribobio) was assessed using the $2 - \Delta\Delta Ct$ method with RNA content normalized to the U6 RNA (Ribobio) and to β-actin for the other genes and plotted (22). The primers for qRT-PCR analysis of SRSF2, E2F1, ABCC8, CASP2S/L, and β-actin expression were synthesized by Invitrogen (supplemental Table S1).

DNA—Genomic DNA was isolated by a standard phenol/chloroform purification method, qualified by electrophoresis on an agarose gel, and visualized with ethidium bromide. For DNA methylation analysis, the primers for methylation-specific PCR (MSP) and bisulfite sequencing PCR (BSP) were designed according to MethPrimer (supplemental Table S1) The methylation status of the miR-193a gene locus was determined by both MSP and BSP as described previously (23).

The CpG methylome was established by probing the heavily methylated DNA fraction enriched by the methylated DNA-binding domain of the rat Mecp2 (24) to the Nimblegen customized CpG island array (0.38 million probes) and validated by bisulfite sequencing as described previously (25). Solexa sequencing-based miR expression profiling was provided by BGI (Shenzhen, China).

In Vivo Study

After transfection with 50 nM miR-193a-3p or mock antagomirs (Ribobio) for 24 h, SMMC-7721 cells were collected and subcutaneously injected into the right and left flanks (1.25×10^6 cells/point) of each nude mouse (10 total), respectively. On day 12 after cell injection, five mice intraperitoneally received 5-FU (75 mg/kg mouse body weight) once per week. The remaining five mice received phosphate-buffered saline (PBS) as a mock treatment control. Also, at the same time, the right sides of all mice tumors were intratumorally injected with 50 nM miR-193a-3p antagomir, and the left sides were injected with mock antagomir (according to the manufacturer's instructions (Ribobio)). To monitor the tumor growth, the volume was measured with a Vernier caliper on days 12, 18, 25, and 32 and calculated as volume $= W^2 \times L \times 0.5$ (where W and L represent the largest and next largest tumor diameters (cm)) and then plotted (26). Mice were humanely sacrificed on day 32, and the tumors were weighed and photographed. Immunostaining (27) was performed for Ki67, SRSF2, and E2F1 expression in both tumors of mouse number 4 (PBS-treated) and mouse number 6 (5-FU-treated).

Expressions of SRSF2, E2F1, and Ki67 proteins were measured by immunochemical analysis on 5-mm slices of formalin-fixed paraffin-embedded tumor xenografts in nude mice. Antigens were retrieved by pretreating dewaxed sections in a microwave oven at 750 watts for 5 min in a citrate buffer (pH 6) and processed with the Super Sensitive Link-Labeled Detection System (Biogenex, Menarini, Florence, Italy). The enzymatic activity was developed by using 3-amino-9-ethylcarbazole (Dako, Milan, Italy) as a chromogenic substrate. Following counterstaining with Mayer hematoxylin (Invitrogen), slides were mounted in aqueous mounting medium (glycergel, Dako). The relative level of each protein was calculated as the density score (mean intensity/lasso, TMAJ density score) that was determined by using TMAJ software (available from the Johns Hopkins Medical Institute Web site), and the percentage of the TMAJ reads of mock over the antagomir-transfected tumor was calculated and plotted.

Statistical Analysis

Data are presented as means, and *error bars* indicate the S.D. or S.E. All statistical analyses were performed with Excel (Microsoft, Redmond, WA) or Prism (GraphPad Software Inc., La Jolla, CA). Two-tailed Student's t test, a one-way analysis of variance or Mann-Whitney U test was used to calculate statistical significance. A p value of <0.05 was considered to be significant.

RESULTS

DNA Methylation-regulated miR-193a-3p Expression Correlates 5-FU Resistance of SMMC-7721 and QGY-7703—The chemoresistance of eight HCC cell lines was determined by IC_{50} profiling: QGY-7703, SMMC-7721, YY-8103, PLC, HepG2, BEL-7402, Hep3B, and FOCUS to gemcitabine, 5-FU, cisplatin, vinorelbine, docetaxel, mitomycin, paclitaxel, irinotecan, and epirubicin, respectively. The IC_{50} difference among HCC cell lines to vinorelbine, docetaxel, mitomycin, paclitaxel, and epirubicin was no more than 17-fold (Fig. 1*A*). However, the IC_{50} to 5-FU of QGY-7703 was ~105.2-fold ($IC_{50} = 0.39$ *versus* 41.01 μg/ml) lower than that of SMMC-7721, whereas their IC_{50} to each of the remaining therapeutics differed little (Fig. 1, *B* and *C*). HepG2 was the second 5-FU-sensitive HCC cell line ($IC_{50} = 1.45$ μg/ml, 27.3-fold lower than SMMC-7721; supplemental Fig. S1*A*) in this group, with the other five members even more resistant to 5-FU than SMMC-7721 (the data of four cell lines are shown in supplemental Fig. S1*B*). Therefore, the genomic profiling at both DNA methylation and miR expression levels was carried out in both QGY-7703 and SMMC-7721 for the DNA methylation regulated miRs having a key role in the 5-FU resistance of HCC cells. Among 39 differentially expressed miRs that were identified by a Solexa sequencing-miRomic analysis,[4] miR-193a-3p was one of the most differentially expressed between SMMC-7721 and QGY-7703: 11.21-fold higher in former than in the latter by Solexa sequencing (Fig. 1*D*) and 4.44-fold higher by qRT-PCR-based validation (Fig. 1*E*). The miR-193a-3p level was also low in another 5-FU-sensitive HCC cell line, HepG2 (the second 5-FU-sensitive cell line), but high in all other 5-FU-resistant cell lines: PLC, FOCUS, Hep3B, and BEL-7402 (supplemental Fig. S1*C*). We also established the methylomic profiles of both cell lines by probing a customized Nimblegene 0.38 million oligonucleotide CpG island array with the heavily methylated DNA fraction from a methylated DNA-binding domain-based capture procedure (28). The miR-193a gene was at the top of the most differentially methylated CpG islands (>3000)[4]: hypermethylated in QGY-7703 and hypomethylated in SMMC-7721 (methylation index, +1.22 *versus* −2.35; Fig. 1*F*), negatively correlating with the miR-193a-3p expression. We further determined the methylation state of the miR-193a gene by BSP and MSP of these two HCC cell lines and the other five HCC cell

[4] K. Ma, Y. He, H. Zhang, Q. Fei, D. Niu, D. Wang, X. Ding, H. Xu, X. Chen, and J. Zhu, unpublished observation.

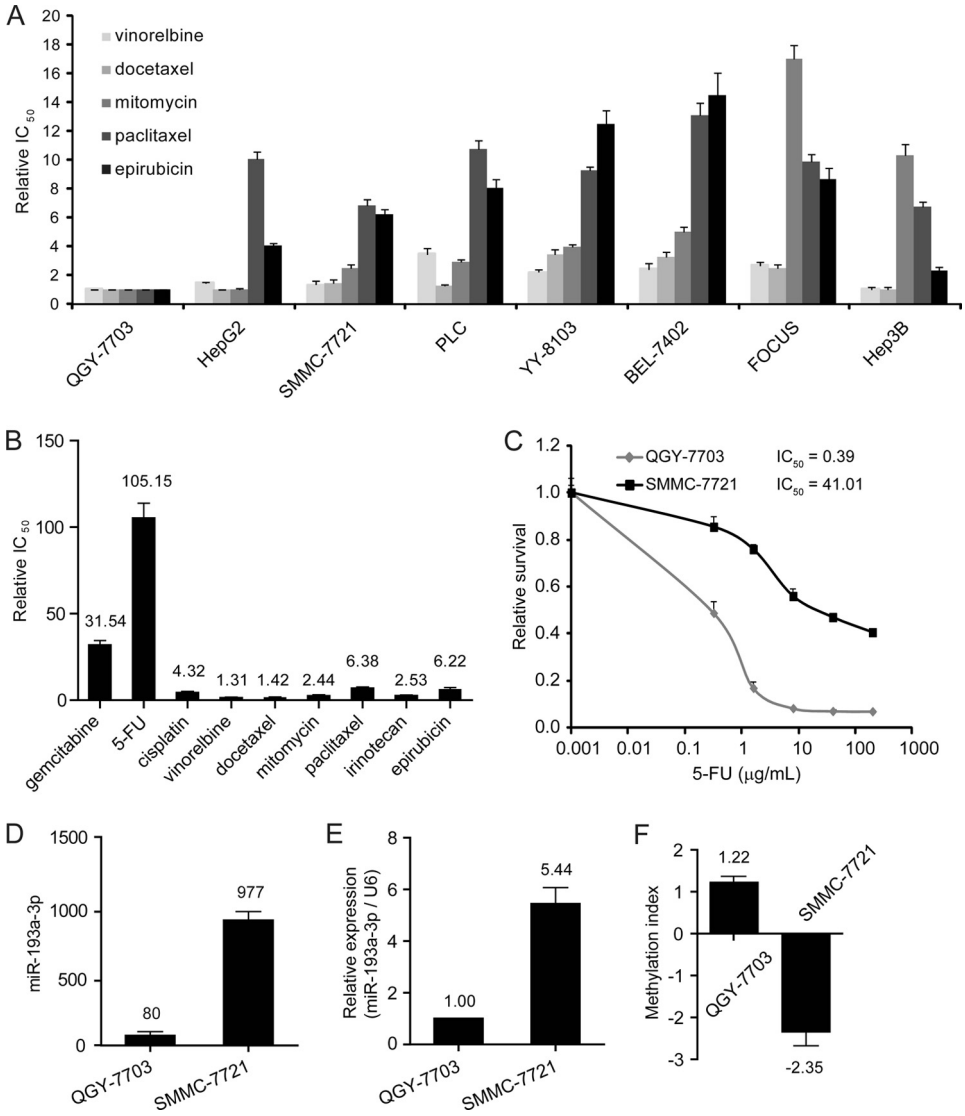

FIGURE 1. **DNA methylation-regulated miR-193a-3p expression correlates 5-FU resistance of SMMC-7721 *versus* QGY-7703.** *A*, relative IC_{50} values (-fold) to each of five chemotherapeutics in each of the other seven HCC cell lines over QGY-7703 were plotted. *B*, relative IC_{50} values to each of nine drugs of SMMC-7721 over QGY-7703 were plotted. *C*, IC_{50} to 5-FU of SMMC-7721 and QGY-7703. The percentage of the relative MTT reads over each 5-FU dose point was calculated and plotted against $\log_{10}$ μg/ml of 5-FU. *D*, miR-193a-3p expression (in reads) was determined by miRomic profiling by using the Solexa sequencing platform. *E*, miR-193a-3p expression was determined by qRT-PCR analysis, digitized with U6 RNA (arbitrarily as 1). *F*, DNA methylation state of the miR-193a gene was determined by an assay combining the methylated DNA-binding domain enrichment of heavily methylated DNA fraction and a CpG island array-based analysis. The methylation index was as follows: >1 = hypermethylated state; <0 = unmethylated state. Error bars, S.D.

lines and showed that miR-193a was hypermethylated in both 5-FU-sensitive cell lines (HepG2 and QGY-7703) but unmethylated or barely methylated in all five of the 5-FU-resistant cell lines, including SMMC-7721 (supplemental Fig. S1, *D–F*). The DNA methylation state dependence of miR-193a transcription was finally confirmed by showing that 5-aza-2′-deoxycytidine-mediated demethylation raised the steady state level of miR-193a-3p in QGY-7703 (supplemental Fig. S2). It is evident that the 5-FU sensitivity of HCC is tightly linked to the DNA methylation-regulated miR-193a-3p expression in HCC.

Both SRSF2 and E2F1 Genes Are Bona Fide Targets of miR-193a-3p—To determine whether differentially expressed miR-193a-3p do have a functional impact, we transfected both cell lines with each of three luciferase reporter constructs: CMV-luc (empty vector control) and its derivatives miR-193a-3p-luc (the testing construct) and miR-127-luc (a nonspecific control). The latter two have each of the cognate target sequences inserted at the 3′-end of the luciferase genes, respectively (Fig. 2*A*). Correlating well with the level of miR-193a-3p, in comparison with each of other reporter, the luciferase activity of the transfected miR-193a-luc was no more than 0.29-fold in SMMC-7721 (a miR-193a-3p high expressing cell line) (Fig. 2*B*), but was similar in QGY-7703 (a miR-193a-3p low expressing cell line) (Fig. 2*C*).

To identify the target gene(s), expression of which is repressed by miR-193a-3p at the post-transcriptional level, we performed Western blot analysis of 10 proteins in both HCC cell lines. The following five proteins were selected from 141 bioinformatically predicted miR-193a-3p target genes (see the TargetScan and EMBL-EBI Web sites): E2F transcription factor 1 (E2F1), E2F transcription factor 6 (E2F6), tyrosine 3-monooxygenase/tryptophan 5-monooxygenase activation protein,

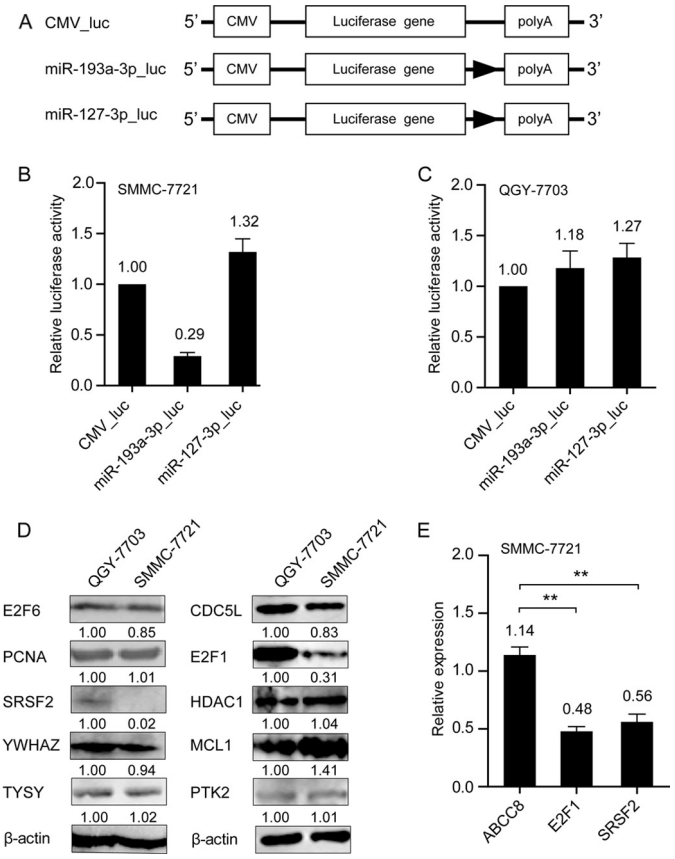

FIGURE 2. **E2F1 and SRSF2 are *bona fide* miR-193a-3p targets.** *A*, the constructs used in this study. CMV promoter-driven construct (CMV_luc) and its derivatives (miR-193a-3p-luc and miR-127-luc) with the target sequences (*filled triangle*) were inserted downstream of the luciferase gene. Each firefly luciferase reporter construct was co-transfected into SMMC-7721 (*B*) and QGY-7703 (*C*) with a *Renilla* luciferase reporter (to control for transfection efficacy). The firefly luciferase activities (mean ± S.D. (*error bars*)) were standardized with the *Renilla* luciferase activities in each transfection, and then the relative activities of each over CMV_luc (set arbitrarily as 1) were plotted. *D*, protein levels by Western blot analysis were digitized with β-actin (arbitrarily as 1). *E*, mRNA levels ($2 - \Delta\Delta Ct$) by qRT-PCR analysis were standardized with β-actin (set arbitrarily as 1), and the ratios of E2F1 and SRSF2 mRNA to ABCC8 mRNA in SMMC-7721 *versus* QGY-7703 were calculated and plotted (**, $p < 0.01$).

ζ-polypeptide (YWHAZ), serine/arginine-rich splicing factor 2 (SRSF2), and myeloid cell leukemia sequence 1 (BCL2-related; MCL1). We also selected thymidylate synthetase for its role in 5-FU metabolism, protein-tyrosine kinase 2 (PTK2) for its role in cell motility and survival, histone deacetylase 1 (HDAC1) for its involvement in protein acetylation regulation, and both proliferating cell nuclear antigen and CDC5 cell division cycle 5-like (CDC5L) for their functional coupling with SRSF2 that is suggested bioinformatically (see the FunCoup Web site). Both SRSF2 and E2F1 (0.02 *versus* 1 and 0.31 *versus* 1, respectively; Fig. 2*D*) but none of the others tested have the expected pattern for a *bona fide* target of miR-193a-3p (*i.e.* low in the miR-193a-3p high expressing SMMC-7721 and high in the miR-193a-3p low expressing QGY-7703). Both mRNA levels were also lower in SMMC-7721 than in QGY-7703 ($2 - \Delta\Delta Ct$ of SMMC-7721/QGY-7703, 0.56 for SRSF2 and 0.48 for E2F1; Fig. 2*E*), in contrast to a similar level of a non-miR-193a-3p target: ATP-binding cassette, subfamily C (CFTR/MRP), member 8 (ABCC8) (1.14; Fig. 2*E*). Taken together, the miR-193a-3p regulation of HCC sensitivity to 5-FU is probably achieved by its regulation of both SRSF2 and E2F1 expression at both mRNA stability and translation levels. The lack of an intercellular difference in thymidylate synthetase level suggested that the 5-FU metabolistic process may not impact the 5-FU resistance of HCC cells in this study.

Forced Alteration of miR-193a-3p Level Reverses 5-FU Resistance of HCC Cells—We raised the miR-193a-3p level by the mimic transfection and found that 1) the luciferase activity of miR-193a-3p-luc was reduced to 0.21-fold (Fig. 3*A*), and 2) both E2F1 and SRSF2 proteins went down to 0.47- and 0.24-fold, respectively, of the mock mimic-transfected levels in QGY-7703 (Fig. 3*C*). We then reduced the miR-193a-3p level by the antagomir transfection and found 1) the luciferase activity of the miR-193a-3p-luc up to 2.43-fold (Fig. 3*B*) and 2) the level of both E2F1 and SRSF2 up to 1.84- and 2.47-fold, respectively, of the mock antagomir transfected levels in SMMC-7721 (Fig. 3*C*). Neither MCL1 nor HDAC (non-target proteins) protein levels were affected by the same treatments (Fig. 3*C*). The changes of SRSF2 and E2F1 mRNAs but not ABCC8 mRNA (a non-target control) were also evident (Fig. 3*D*), indicating the involvement of miR-193a-3p-mediated control of the mRNA stability level. The miR-193a-3p mimic transfection also slowed down QGY-7703 cell proliferation by 27% (1.05 *versus* 1.44 for the mock, $p = 0.0227$; Fig. 4, *A* and *C*) and induced G_1 arrest in QGY-7703 (G_1 phase 62.76 *versus* 50.71% for the mock; Fig. 4*D*). More importantly, its 5-FU IC_{50} of was raised by 6.35-fold (5.29 *versus* 0.72 μg/ml; Fig. 4*E*) in comparison with the mock mimic transfected control. SRSF2 responds more profoundly than E2F1 to the changing level of miR-193a-3p (Fig. 3). In view of the fact that SRSF2 is a direct target of E2F1 transcriptional regulation (29). We repressed SRSF2 by siRNA in QGY-7703 to assess the role of SRSF2 in the 5-FU resistance of HCC. Consistent with its reduction down to the 0.13-fold level in the mock siRNA transfected control (Fig. 4*B*), QGY-7703 cell proliferation slowed down by 37% (0.66 *versus* 1.04, $p = 0.0323$; Fig. 4*C*), arrested at G_1 phase (G_1 phase 58.33 *versus* 50.11%, $p = 0.0189$, Fig. 4*D*), and became more resistant to 5-FU (IC_{50} of 5-FU, 2.22 *versus* 0.68 μg/ml; Fig. 4*E*). Further confirmation came from the experiment with the miR-193a-3p antagomir-transfected SMMC-7721. In agreement with the 0.63-fold elevation of luciferase activity of co-transfected miR-193a-3p-luc (supplemental Fig. S3*A*), SMMC-7721 cell proliferation was accelerated by 33% (1.88 *versus* 1.41, $p = 0.0479$, supplemental Fig. S3*B*), and more cells entered S phase (G_1 phase 51.3 *versus* 46.6% mock, $p = 0.0362$, supplemental Fig. S3*C*). Most importantly, its 5-FU IC_{50} was reduced by 2.47-fold (46.70 *versus* 13.44 μg/ml, $p = 0.0251$; supplemental Fig. S3*D*). In conclusion, SRSF2 contributes a great deal to miR-193a-3p negative control of HCC resistance to 5-FU.

SRSF2-mediated Elevation in the Ratio of Proapoptotic/Antiapoptotic Forms of Caspase 2 Transcripts Underlies 5-FU Sensitivity in HCC Cells—It has been suggested that relative levels of the proapoptotic/antiapoptotic splicing forms of apoptotic genes rather than the absolute level of either reflects the apoptotic propensity and therefore chemoresistance of cancer cells (30). As a key component of the spliceosome (31), SRSF2 preferentially up-regulate the proapoptotic splice forms of apopto-

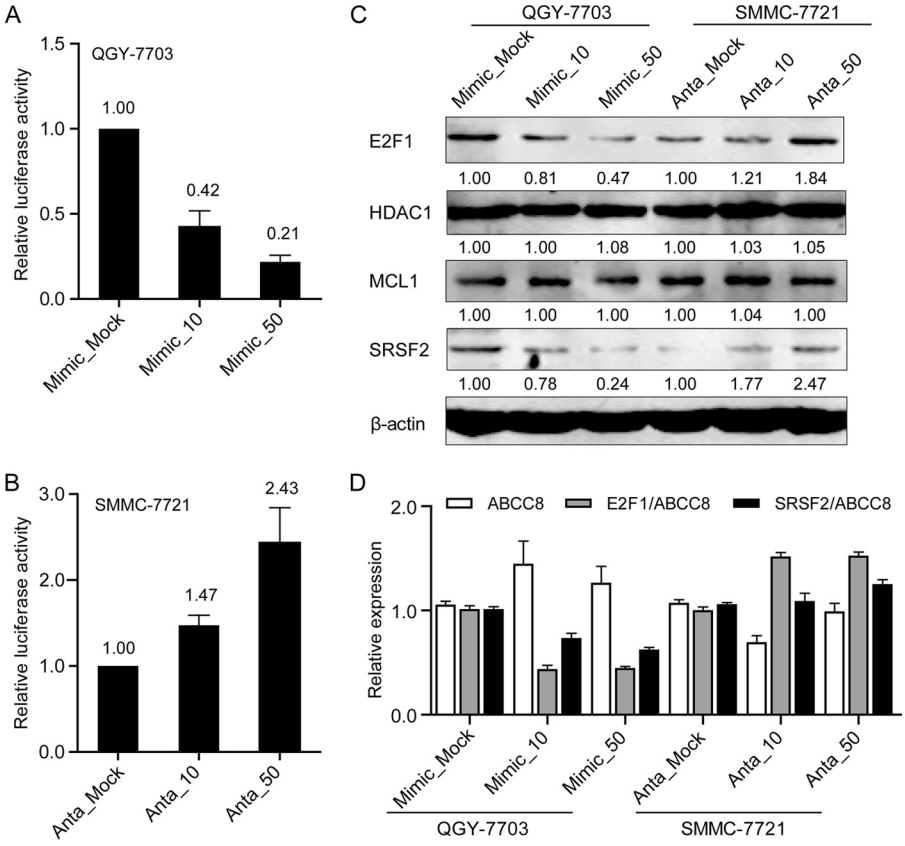

FIGURE 3. **E2F1 and SRSF2 levels are negatively regulated by miR-193a-3p.** QGY-7703 (*A*) and SMMC-7721 (*B*) were transfected with miR-193a-3p mimic (10 and 50 nM), antagomir (10 and 50 nM), or mock control (nonspecific, 50 nM) together with miR-193a-3p-luc, and luciferase activities were determined. Relative luciferase activities over the mock (set arbitrarily as 1) were calculated. *C*, the protein levels of E2F1, SRSF2, HDAC1, MCL1, and β-actin in mock- and mimic-transfected (QGY-7703) or antagomir-transfected (SMMC-7721) cells were compared by Western blot and digitized with that in the mock-transfected cells (arbitrarily as 1). *D*, the mRNA levels of E2F1, SRSF2, and ABCC8 were determined by qRT-PCR analysis and digitized with ABCC8 (set arbitrarily as 1). *Error bars*, S.D.

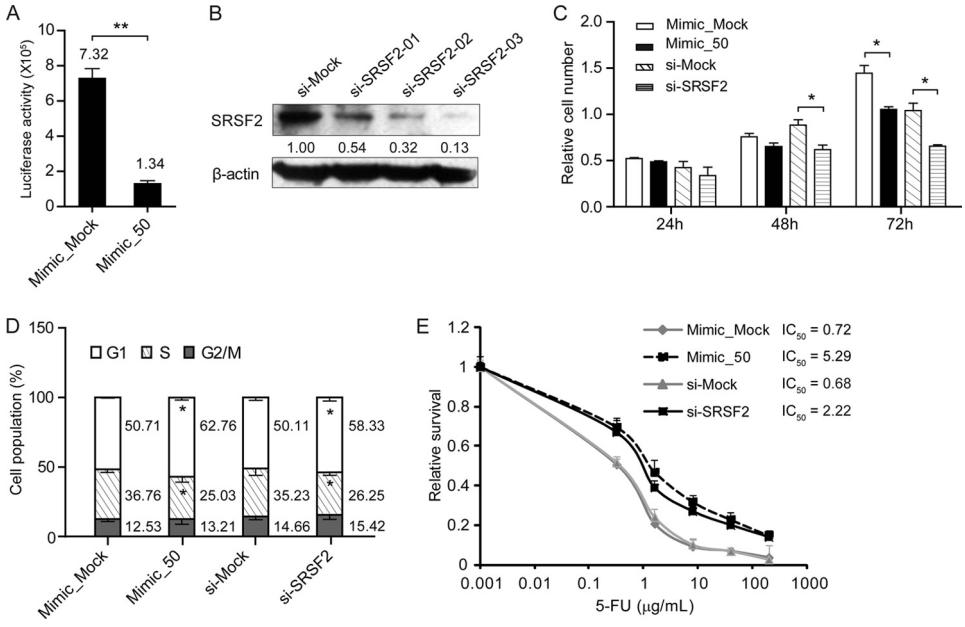

FIGURE 4. **Down-regulation of SRSF2 by miR-193a-3p mimic or siRNA transfection slowed down cell proliferation, caused G_1 arrest, and raised 5-FU resistance of QGY-7703.** *A*, miR-193a-3p (50 nM; *Mimic_50*) or unrelated mimic (mock, 50 nM; *Mimic_mock*) was co-transfected with miR-193a-3p-luc into QGY-7703, and luciferase activities were measured and plotted. *B*, SRSF2 levels in the siRNA-01, -02, and -03 or the mock siRNA-transfected QGY-7703 were compared by Western blot analysis at 48 h after transfection. *C*, cell numbers were determined by MTT assays at 24, 48, and 72 h after transfection of the miR-193a-3p mimic and Mimic_mock, the SRSF2 siRNA_03 (*si_SRSF2*), and mock siRNA (*si-Mock*) into QGY-7703, respectively. *D*, cycle phase distributions (percentage) were determined by FACS analysis and plotted. *E*, IC_{50} to 5-FU values were determined by MTT assays and plotted (*, $p < 0.05$; **, $p < 0.01$). *Error bars*, S.D.

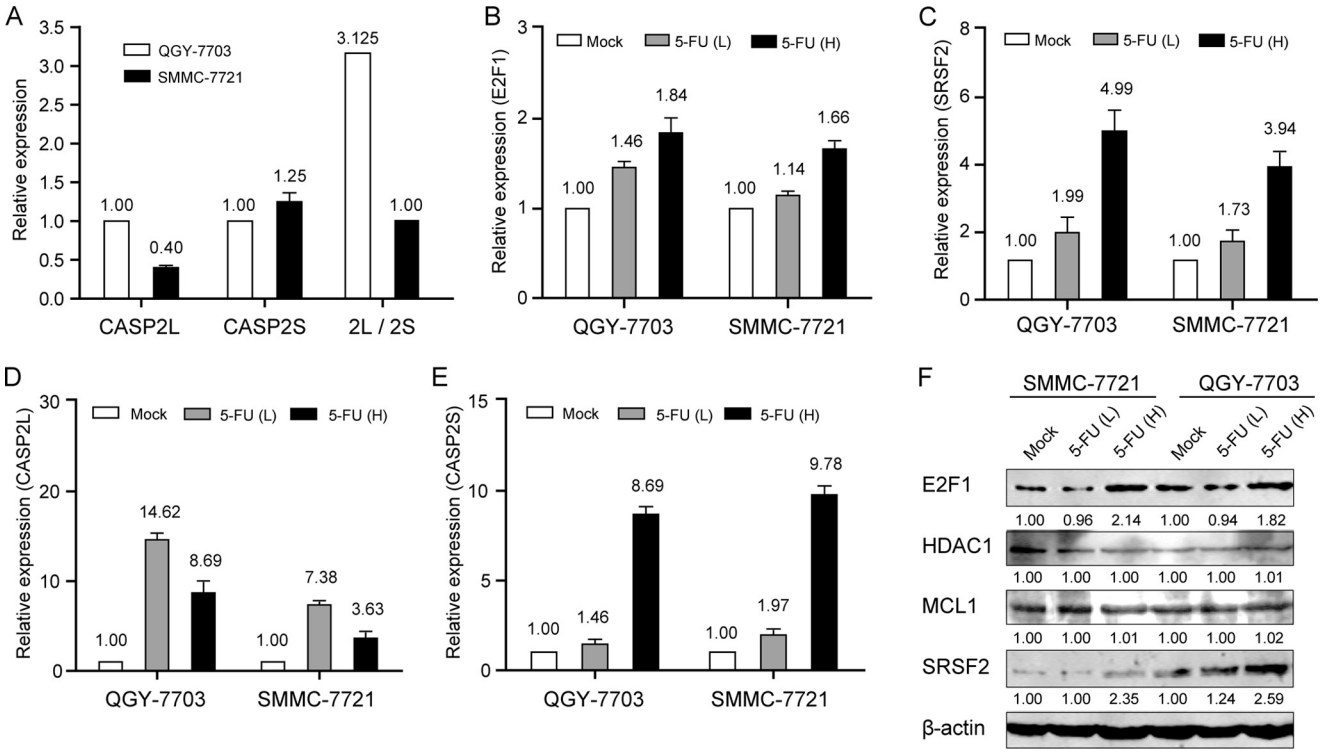

FIGURE 5. **5-FU raises the expression of E2F1, SRSF2, and the proapoptotic splice form of caspase 2 in both cell lines.** *A*, the mRNA levels of both CASP2L (proapoptotic splicing form) and CASP2S (antiapoptotic splicing form) of caspase 2 in both QGY-7703 (*open column*) and SMMC-7721 (*filled column*) were quantified by qRT-PCR and compared. The effects of 5-FU on the mRNA levels of E2F1 (*B*), SRSF2 (*C*), CASP2L (*D*), and CASP2S (*E*) in mock- and 5-FU-treated cells were assessed at 24 h after treatment with a low dose (4 μg/ml 5-FU (*L*)) or a high dose (300 μg/ml 5-FU (*H*)) and then with mock control (set arbitrarily as 1). *F*, the protein levels of E2F1, SRSF2, HDAC1, MCL1, and β-actin in the mock- and 5-FU-treated cells were examined by Western blot.

tic genes, including CASP8 and FADD-like apoptosis regulator (*C-Flip*); caspase 8 and 9, apoptosis-related cysteine peptidase (*Caspase 8* and *9*); and apoptosis regulator Bcl-X (*Bcl-x*) (29). To test this notion, we quantified the steady-state level of both proapoptotic (CASP2L) and antiapoptotic (CASP2S) forms of caspase 2 mRNAs in both cell lines by qRT-PCR. Positively correlating with the SRSF2 level, the CASP2L level in QGY-7703 was 1.5-fold higher than that in SMMC-7721, and the level of proapoptotic and antiapoptotic CASP2S was 0.25-fold lower than in SMMC-7721 cells. Taking both measurements into consideration, the ratio of the CASP2L/CASP2S mRNA level in QGY-7703 was 2.125-fold higher than in SMMC-7721 (Fig. 5*A*). In light of all that is known so far, this ratio is very likely to be a most robust indicator of the 5-FU resistance of HCC. To determine the 5-FU impact in this system, we treated both cell lines by 4 μg/ml (a low dose) and 300 μg/ml (a high dose) for 1 day, respectively. Neither cell lines showed any sickness under a microscope even after a high dose of 5-FU treatment. As expected, both RNA and protein of SRSF2 were elevated by a larger margin than E2F1 in both QGY-7703 and SMMC-7721 (Fig. 5, *B*, *C*, and *F*). Compatible with the extent of the SRSF2 up-regulation by a low dose of 5-FU, CASP2L RNA (14.62- and 7.38-fold the untreated level in QGY-7703 and SMMC-7721, respectively) was more drastically up-regulated than CASP2S (1.46- and 1.97-fold the untreated levels) in both cell lines (Fig. 5, *D* and *E*). However, both CASP2S and CASP2L mRNAs were raised by a high dose 5-FU by a similar extent in both cell lines (Fig. 5, *D* and *E*). We also conclude that the intercellular difference (3.125-fold) of the CASP2L/CASP2S mRNA level was preferentially enlarged by 5-FU treatment, particularly for a low dose.

Antagomir-mediated Suppression of miR-193a-3p Inhibited Tumor Growth and Potentiated 5-FU Sensitivity of SMMC-7721 in Nude Mice—We then compared the tumorigenicity of QGY-7703 and SMMC-7721 in nude mice. Whereas subcutaneous injection of 7.5×10^6 QGY-7703 cells/point produced no visible tumor mass 2 weeks after the injection, 1.25×10^6 SMCC-7721 cells/point (one-fifth of the dose of QGY-7703) resulted in visible tumor growth (not shown). This indicated that miR-193a-3p expression also involves the HCC tumorigenicity.

SMMC-7721 cells were batch-transfected with the miR-193a-3p antagomir and mock antagomir, and both SRSF2 and E2F1 protein levels were determined (Fig. 6*A*). Cells were subcutaneously injected into the right and left flanks of nude mice, respectively. Five mice were subjected to 5-FU or PBS administration on days 18 and 25, respectively. At the same time, the antagomir and mock were respectively intratumorally injected into the corresponding sides of all 10 mice (Fig. 6*B*). The tumor volume of the antagomir-transfected tumor was significantly smaller than that of the mock antagomir-transfected one on day 12 (0.05 *versus* 0.2 cm^3, $p = 0.032$), on day 25 (0.13 *versus* 0.45 cm^3, $p = 0.039$), and on day 32 (0.65 *versus* 1.03 cm^3) (Fig. 6*C*), and the tumor mass of the antagomir treated were lighter than that of the mock treated mice on day 32 (0.71 *versus* 1.14 g, Fig. 6*D*). 5-FU administration showed little effect on tumor

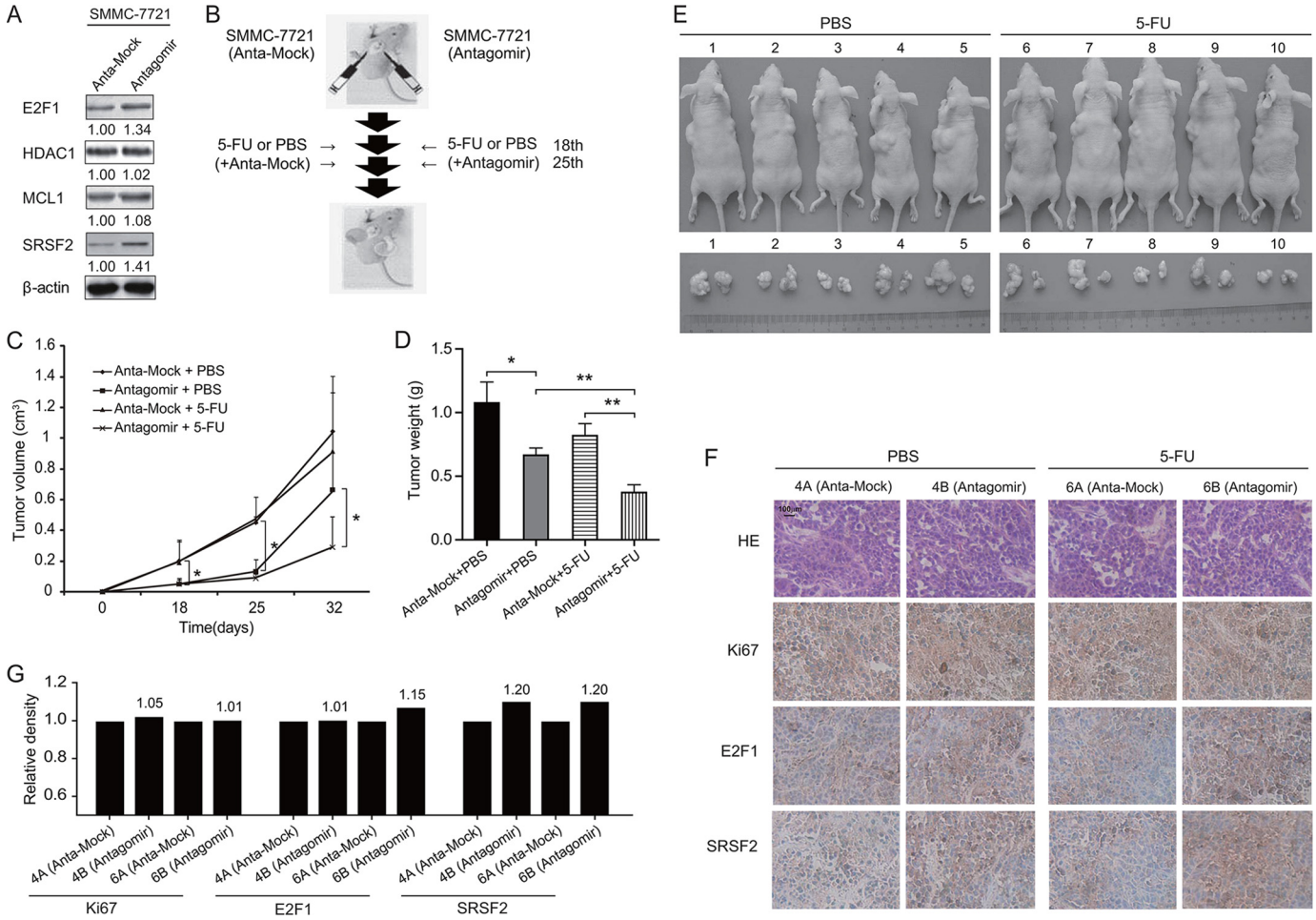

FIGURE 6. **Antagomir-mediated repression of miR-193a-3p inhibited tumor growth and sensitized SMMC-7721 to 5-FU in nude mice.** *A*, SRSF2, E2F1, HDAC1, and MCL1 proteins were determined by Western blot analysis in the batch of antagomir- and mock-transfected SMMC-7721 cells after a 48-h transfection. *B*, then the cells (at a dose of 1.25×10^6 cells/point) were subcutaneously injected into both flanks of nude mice as follows: mock antagomir-transfected on the left flank and the antagomir-transfected on the right flank and 5-FU or PBS and antagomir or mock (*Anta-mock*) were given on days 18 and 25. *C*, tumor volume (mean ± S.D. (*error bars*)) was measured with a Vernier caliper on days 18, 25, and 32 and compared. *D* and *E*, mice were humanely killed on day 32, and the tumors were photographed and weighed (*, $p < 0.05$; **, $p < 0.01$). *F*, levels of Ki67, SRSF2, and E2F1 proteins in tumor tissues of mouse 4 (PBS-treated) and mouse 6 (5-FU-treated) were determined by immunostaining. *G*, the level of each protein was quantified as the mean density of the whole area in each slide by using TMAJ software, and then the relative density of mock-*versus* antagomir-treated mice was calculated and plotted (*, $p < 0.05$; **, $p < 0.01$).

growth in the mock-transfected SMMC-7721 cells. For PBS *versus* 5-FU, tumor volume was as follows: on day 25, 0.46 *versus* 0.45 cm^3; on day 32, 1.03 *versus* 0.89 cm^3 (Fig. 6*C*). Tumor weight on day 32 was 1.14 *versus* 0.82 g (Fig. 6*D*). However, 5-FU had a significant impact on tumor growth in the antagomir-treated SMMC-7721 cells: tumor volume on day 32, 0.65 *versus* 0.29 cm^3 ($p = 0.0427$) (Fig. 6*C*); tumor weight on day 32, 0.71 *versus* 0.37 g ($p = 0.0084$) (Fig. 6*D*). The further confirmation of the key role of miR-193a-3p in 5-FU resistance of HCC came from the immunostaining analysis of SRSF2, E2F1, and Ki67 (an indicator for cell proliferation) in the tumor session from 5-FU-treated (number 6) and PBS-treated (number 4) mice. As expected, antagomir treatment raised the SRSF2 level by 20% in tumor xenografts on day 32, regardless of 5-FU administration (Fig. 6, *F* and *G*). However, a 20% elevation of E2F1 was evident only in 5-FU/antagomir-treated and not in any other cases, suggesting different roles and mechanisms between E2F1 and SRSF2 in the dictation by miR-193a-3p of HCC 5-FU resistance.

DISCUSSION

Our knowledge about cancer has been rapidly expanded for last few decades. However, our ability to control this threatening disease has only been marginally improved, because a patient's survival today is only marginally prolonged compared with 40 years ago. A lack of effective measures for early detection and/or accurate stratification of the disease have been largely blamed. Requirement of companion diagnostics by the United States Food and Drug Administration for approval of newly developed drugs will soon be introduced (32), highlighting the increasing appreciation of the urgent need for robust cancer diagnostics. Among all of the biological indicators evaluated, two epigenetic identities, DNA methylation and miRs, have garnered a great deal of attention recently, for their greater potential to achieve better detection and staging of cancer in clinic. Akin to the protein-coding genes, some miR genes are transcriptionally repressed by the hypermethylated states of their promoters, particularly for those collocated with the

CpG-rich regions in the genome. On the other hand, the expression of DMNT3B, a key regulator of DNA methylation in mammalian cells, is also subjected to regulation by the miR-29 cluster at the level of translation (33). It is desirable, therefore, to define the molecular details for HCC chemoresistance (5-FU in this study) from both DNA methylation and miR perspectives rather than from each independently.

In this study, we carried out IC_{50} profiling of eight HCC cell lines to nine common chemotherapeutics and chose QGY-7703 as a 5-FU-sensitive and SMMC-7721 as a resistant cell line for the genomic screening at both DNA methylation and miRomic levels for the corresponding differences that are specific to HCC 5-FU resistance (Fig. 1, *A* and *B*, and supplemental Fig. S1*A*). Tight association of DNA methylation-regulated miR-193a-3p expression with HCC 5-FU resistance was first suggested by genomic studies (Fig. 1) and then independently confirmed by qRT-PCR of miR-193a expression and DNA methylation analysis (BSP and MSP) in this pair of HCC cell lines (Fig. 1 and supplemental Figs. S1*A* and 2) and another 5-FU-sensitive cell line, HepG2, and four more resistant cell lines, PLC, BEL-7402, Hep3B, and FOCUS (supplemental Fig. S1, *A–F*). Therefore, the miR-193a-3p-centered mechanistic insights detailed by the systematic studies of QGY-7703 and SMMC-7721 are truly specific to 5-FU resistance of HCC. Forced reversion of the miR-193a-3p level in both cell lines has turned around phenotypic features tested: the expression of the target genes (Figs. 2 and 3), cell proliferation, cell cycling profile, and 5-FU sensitivity (Fig. 4 and supplemental Fig. S3). The conclusion was further supported by the observation from the *in vivo* studies that repression of the miR-193a-3p level by antagomir technologies repressed tumor growth and sensitized SMMC-7721 cells to 5-FU (Fig. 6). For the key mediators downstream of miR-193a-3p, we compared both protein and mRNA levels of five bioinformatically predicted miR-193a-3p targets in both cell lines, SRSF2 and E2F1, but none of the others met the expectation: higher in QGY-7703 and lower in SMMC-7721 cells (Fig. 2). Importantly, siRNA-mediated repression of SRSF2 phenocopied all of the biological changes in the miR-193a-3p mimic-transfected QGY-7703 (Fig. 4). Up-regulated expression of SRSF2 was also evident in the SMMC-7721-derived tumor xenograft by the antagomir transfection (Fig. 6, *F* and *G*). Thus, SRSF2 relays miR-193a-3p regulation (upstream regulator) by raising the ratio of proapoptotic *versus* antiapoptotic splicing of the caspase 2 to dictate the HCC tumorigenicity and 5-FU resistance (Fig. 7).

Deregulation of the E2F transcription factors is a hallmark of cancer, often indicative of a poor prognosis (34). E2F1 controls transcription of multiple genes, each directly or indirectly involved in the regulation of G_1-S phase entry (cell proliferation) or apoptosis of cells (35, 36). E2F1 activation triggered by DNA damage often accompanies with the favorable changes in its chemical modification state and its interaction state with the retinoblastoma protein (37). As an E2F1 target, SRSF2 transcription is also up-regulated in the stressed cell and consequently raises the ratio of the proapoptotic to the antiapoptotic splicing form of the apoptotic genes (29). In this study, we showed for the first time that both SRSF2 and E2F1 are *bona fide* targets of miR-193a-3p (Fig. 2). Therefore, repression of

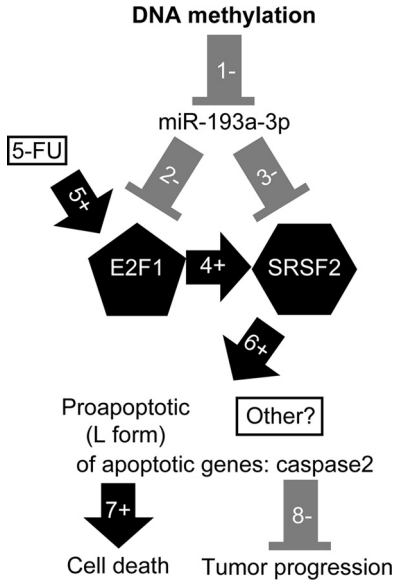

FIGURE 7. **A model for mechanism of action.** Expression of miR-193a-3p is suppressed by the hypermethylated state of its promoter (*1*−). miR-193a-3p suppresses both E2F1 and SRSF2 expression at the post-transcriptional levels (*2*− and *3*−). The function of E2F1 is activated by 5-FU treatment (5+), which activates the transcription and therefore activity of SRSF2 (*4*+). SRSF2 preferentially up-regulates the proapoptotic splicing form (*6*+) to the antiapoptotic splicing form of caspase 2 transcripts, potentiating cell death (*7*+). It is quite possible for the involvement of the other genes under SRSF2 regulation at the alternative mRNA splicing level to be in control of 5-FU chemoresistance and the *in vivo* tumor growth (*8*−).

SRSF2 expression by miR-193a-3p consists of both direct and indirect components. The E2F1-mediated component explains well why the SRSF2 always responds more profoundly than E2F1 to the change of miR-193a-3p level in cells (Figs. 2–6 and supplemental Fig. S3). The genotoxic insults may also trigger both phosphorylation and acetylation and changes in SRSF2 activity (38), representing an E2F1-independent pathway for SRSF2 activation in the DNA-damaged cells. SRSF2 is a key member of a serine/arginine-rich protein family that regulates constitutive and alternative pre-mRNA splicing for extensive diversities in gene expression that are evident across tissues, developmental stages, and diseases (39). Multiple forms of protein are often generated from a single primary transcript, having different and even opposite functions (39). The eminent examples in the cancer field are proapoptotic *versus* antiapoptotic isoforms of the caspase genes (29) as well as prooncogenic *versus* antioncogenic isoforms of BRCA1 (40) and CD44 (41). The aberrant RNA splicing in cancer has been attributed to the mutations in *cis*-motifs to both genetic defects (42) and aberrant expression (43) of the protein components of the mRNA splicing machinery. The stressed cells often have a high level of both RNA splicing activity (44) and the proapoptotic form of the apoptotic genes (29). Consistent with this, the ratio of the proapoptotic/antiapoptotic forms of the caspase 2 transcript in 5-FU-sensitive QGY-7703 is higher than that in resistant SMMC-7721 (Fig. 5) and rose in the 5-FU-treated HCC cells (Fig. 5). Therefore, in comparison with other events, this ratio is a better indicator for both 5-FU resistance and tumorigenicity of HCC.

Several molecular events have been implicated in the 5-FU resistance of cancer cells. For instance, the association of the

overexpressed astrocyte elevated gene-1 (AEG-1) with 5-FU resistance of HCC cells was ascribed to the ability of AEG-1 to activate the transcription the genes that catabolize 5-FU (45). Other indicators for resistance of cancer cells to 5-FU include dysregulated Ep-CAM (46), Hsp27, and Hsp40 proteins (47). miR-21 represses hMSH2 expression (26), which was reported to be overexpressed in colorectal cancers that are refractory to 5-FU therapy. Taken together, we showed for the first time that miR-193a-3p regulates the 5-FU resistance of HCC, and its transcription is repressed by the hypermethylated promoter state. Both SRSF2 and E2F1 are true targets of miR-193a-3p, and SRSF2 is the key mediator to dictate the 5-FU resistance in HCC. Both tumorigenicity and 5-FU resistance of HCC cells are directly associated with the ability of SRSF2 to elevate the ratio of the proapoptotic/antiapoptotic forms of the caspase 2 transcript. Finally, the observation detailed in this report suggests a list of novel candidates as prognostic indicators for rational 5-FU therapy of HCC: DNA methylation state or the levels of miR-193a-3p, SRSF2, E2F1, and the proapoptotic form of caspase 2.

Acknowledgments—We thank Yi Zhang for advice on SRSF2 involvement in this study and Moshe Szyf for critical reading of the manuscript.

REFERENCES

1. Salk, J. J., Fox, E. J., and Loeb, L. A. (2010) Mutational heterogeneity in human cancers. Origin and consequences. *Annu. Rev. Pathol.* **5,** 51–75
2. Irizarry, R. A., Ladd-Acosta, C., Wen, B., Wu, Z., Montano, C., Onyango, P., Cui, H., Gabo, K., Rongione, M., Webster, M., Ji, H., Potash, J. B., Sabunciyan, S., and Feinberg, A. P. (2009) The human colon cancer methylome shows similar hypo- and hypermethylation at conserved tissue-specific CpG island shores. *Nat. Genet.* **41,** 178–186
3. Maher, C. A., Kumar-Sinha, C., Cao, X., Kalyana-Sundaram, S., Han, B., Jing, X., Sam, L., Barrette, T., Palanisamy, N., and Chinnaiyan, A. M. (2009) Transcriptome sequencing to detect gene fusions in cancer. *Nature* **458,** 97–101
4. Bonnette, M. D., Pavlova, V. R., Rodier, D. N., Thompson, L. P., Boone, E. L., Brown, K. L., Meyer, K. M., Trevino, M. B., Champagne, J. R., and Cruz, T. D. (2009) dcDegenerate oligonucleotide primed-PCR for multilocus, genome-wide analysis from limited quantities of DNA. *Diagn. Mol. Pathol.* **18,** 165–175
5. Lin, Q., Geng, J., Ma, K., Yu, J., Sun, J., Shen, Z., Bao, G., Chen, Y., Zhang, H., He, Y., Luo, X., Feng, X., and Zhu, J. (2009) RASSF1A, APC, ESR1, ABCB1 and HOXC9, but not p16INK4A, DAPK1, PTEN and MT1G genes were frequently methylated in the stage I non-small cell lung cancer in China. *J. Cancer Res. Clin. Oncol.* **135,** 1675–1684
6. Fabbri, M., Garzon, R., Cimmino, A., Liu, Z., Zanesi, N., Callegari, E., Liu, S., Alder, H., Costinean, S., Fernandez-Cymering, C., Volinia, S., Guler, G., Morrison, C. D., Chan, K. K., Marcucci, G., Calin, G. A., Huebner, K., and Croce, C. M. (2007) MicroRNA-29 family reverts aberrant methylation in lung cancer by targeting DNA methyltransferases 3A and 3B. *Proc. Natl. Acad. Sci. U.S.A.* **104,** 15805–15810
7. Lujambio, A., Ropero, S., Ballestar, E., Fraga, M. F., Cerrato, C., Setién, F., Casado, S., Suarez-Gauthier, A., Sanchez-Cespedes, M., Git, A., Spiteri, I., Das, P. P., Caldas, C., Miska, E., and Esteller, M. (2007) Genetic unmasking of an epigenetically silenced microRNA in human cancer cells. *Cancer Res.* **67,** 1424–1429
8. Saito, Y., Liang, G., Egger, G., Friedman, J. M., Chuang, J. C., Coetzee, G. A., and Jones, P. A. (2006) Specific activation of microRNA-127 with downregulation of the proto-oncogene BCL6 by chromatin-modifying drugs in human cancer cells. *Cancer Cell* **9,** 435–443
9. Yang, H., Kong, W., He, L., Zhao, J. J., O'Donnell, J. D., Wang, J., Wenham, R. M., Coppola, D., Kruk, P. A., Nicosia, S. V., and Cheng, J. Q. (2008) MicroRNA expression profiling in human ovarian cancer. miR-214 induces cell survival and cisplatin resistance by targeting PTEN. *Cancer Res.* **68,** 425–433
10. Fabbri, M., and Calin, G. A. (2010) Epigenetics and miRNAs in human cancer. *Adv. Genet.* **70,** 87–99
11. Brase, J. C., Wuttig, D., Kuner, R., and Sültmann, H. (2010) Serum microRNAs as non-invasive biomarkers for cancer. *Mol. Cancer* **9,** 306
12. Jemal, A., Center, M. M., DeSantis, C., and Ward, E. M. (2010) Global patterns of cancer incidence and mortality rates and trends. *Cancer Epidemiol Biomarkers Prev.* **19,** 1893–1907
13. Lencioni, R. (2010) Loco-regional treatment of hepatocellular carcinoma. *Hepatology* **52,** 762–773
14. Villanueva, A., Minguez, B., Forner, A., Reig, M., and Llovet, J. M. (2010) Hepatocellular carcinoma. Novel molecular approaches for diagnosis, prognosis, and therapy. *Annu. Rev. Med.* **61,** 317–328
15. Abou-Alfa, G. K., Johnson, P., Knox, J. J., Capanu, M., Davidenko, I., Lacava, J., Leung, T., Gansukh, B., and Saltz, L. B. (2010) Doxorubicin plus sorafenib vs doxorubicin alone in patients with advanced hepatocellular carcinoma. A randomized trial. *JAMA* **304,** 2154–2160
16. Lachenmayer, A., Alsinet, C., Chang, C. Y., and Llovet, J. M. (2010) Molecular approaches to treatment of hepatocellular carcinoma. *Dig. Liver Dis.* **42,** Suppl. 3, S264–S272
17. Yoo, B. K., Emdad, L., Su, Z. Z., Villanueva, A., Chiang, D. Y., Mukhopadhyay, N. D., Mills, A. S., Waxman, S., Fisher, R. A., Llovet, J. M., Fisher, P. B., and Sarkar, D. (2009) Astrocyte elevated gene-1 regulates hepatocellular carcinoma development and progression. *J. Clin. Invest.* **119,** 465–477
18. He, L., Isselbacher, K. J., Wands, J. R., Goodman, H. M., Shih, C., and Quaroni, A. (1984) Establishment and characterization of a new human hepatocellular carcinoma cell line. *In Vitro* **20,** 493–504
19. Fontana, L., Fiori, M. E., Albini, S., Cifaldi, L., Giovinazzi, S., Forloni, M., Boldrini, R., Donfrancesco, A., Federici, V., Giacomini, P., Peschle, C., and Fruci, D. (2008) Antagomir-17–5p abolishes the growth of therapy-resistant neuroblastoma through p21 and BIM. *PLoS One* **3,** e2236
20. Andrisano, V., Bartolini, M., Gotti, R., Cavrini, V., and Felix, G. (2001) Determination of inhibitors' potency (IC50) by a direct high-performance liquid chromatographic method on an immobilised acetylcholinesterase column. *J. Chromatogr. B Biomed. Sci. Appl.* **753,** 375–383
21. Wu, J. Y., and Maniatis, T. (1993) Specific interactions between proteins implicated in splice site selection and regulated alternative splicing. *Cell* **75,** 1061–1070
22. Song, B., Wang, Y., Xi, Y., Kudo, K., Bruheim, S., Botchkina, G. I., Gavin, E., Wan, Y., Formentini, A., Kornmann, M., Fodstad, O., and Ju, J. (2009) Mechanism of chemoresistance mediated by miR-140 in human osteosarcoma and colon cancer cells. *Oncogene* **28,** 4065–4074
23. Yu, J., Zhu, T., Wang, Z., Zhang, H., Qian, Z., Xu, H., Gao, B., Wang, W., Gu, L., Meng, J., Wang, J., Feng, X., Li, Y., Yao, X., and Zhu, J. (2007) A novel set of DNA methylation markers in urine sediments for sensitive/specific detection of bladder cancer. *Clin. Cancer Res.* **13,** 7296–7304
24. Meenhuis, A., van Veelen, P. A., de Looper, H., van Boxtel, N., van den Berge, I. J., Sun, S. M., Taskesen, E., Stern, P., de Ru, A. H., van Adrichem, A. J., Demmers, J., Jongen-Lavrencic, M., Löwenberg, B., Touw, I. P., Sharp, P. A., and Erkeland, S. J. (2011) MiR-17/20/93/106 promote hematopoietic cell expansion by targeting sequestosome 1-regulated pathways in mice. *Blood* **118,** 916–925
25. Li, Y., Zhu, J., Tian, G., Li, N., Li, Q., Ye, M., Zheng, H., Yu, J., Wu, H., Sun, J., Zhang, H., Chen, Q., Luo, R., Chen, M., He, Y., Jin, X., Zhang, Q., Yu, C., Zhou, G., Sun, J., Huang, Y., Zheng, H., Cao, H., Zhou, X., Guo, S., Hu, X., Li, X., Kristiansen, K., Bolund, L., Xu, J., Wang, W., Yang, H., Wang, J., Li, R., Beck, S., Wang, J., and Zhang, X. (2010) The DNA methylome of human peripheral blood mononuclear cells. *PLoS Biol.* **8,** e1000533
26. Valeri, N., Gasparini, P., Braconi, C., Paone, A., Lovat, F., Fabbri, M., Sumani, K. M., Alder, H., Amadori, D., Patel, T., Nuovo, G. J., Fishel, R., and Croce, C. M. (2010) MicroRNA-21 induces resistance to 5-fluorouracil by down-regulating human DNA MutS homolog 2 (hMSH2). *Proc. Natl. Acad. Sci. U.S.A.* **107,** 21098–21103
27. Kantar, M., Kosova, B., Cetingul, N., Gumus, S., Toroslu, E., Zafer, N.,

Topcuoglu, N., Aksoylar, S., Cinar, M., Tetik, A., and Eroglu, Z. (2009) Methylenetetrahydrofolate reductase C677T and A1298C gene polymorphisms and therapy-related toxicity in children treated for acute lymphoblastic leukemia and non-Hodgkin lymphoma. *Leuk. Lymphoma* **50,** 912–917
28. Brinkman, A. B., Simmer, F., Ma, K., Kaan, A., Zhu, J., and Stunnenberg, H. G. (2010) Whole-genome DNA methylation profiling using MethylCap-seq. *Methods* **52,** 232–236
29. Merdzhanova, G., Edmond, V., De Seranno, S., Van den Broeck, A., Corcos, L., Brambilla, C., Brambilla, E., Gazzeri, S., and Eymin, B. (2008) E2F1 controls alternative splicing pattern of genes involved in apoptosis through upregulation of the splicing factor SC35. *Cell Death Differ.* **15,** 1815–1823
30. Schwerk, C., and Schulze-Osthoff, K. (2005) Regulation of apoptosis by alternative pre-mRNA splicing. *Mol. Cell* **19,** 1–13
31. Chen, T., and Li, E. (2006) Establishment and maintenance of DNA methylation patterns in mammals. *Curr. Top. Microbiol. Immunol.* **301,** 179–201
32. Hamburg, M. A., and Collins, F. S. (2010) The path to personalized medicine. *N. Engl. J. Med.* **363,** 301–304
33. Benetti, R., Gonzalo, S., Jaco, I., Muñoz, P., Gonzalez, S., Schoeftner, S., Murchison, E., Andl, T., Chen, T., Klatt, P., Li, E., Serrano, M., Millar, S., Hannon, G., and Blasco, M. A. (2008) A mammalian microRNA cluster controls DNA methylation and telomere recombination via Rbl2-dependent regulation of DNA methyltransferases. *Nat. Struct. Mol. Biol.* **15,** 268–279
34. Timmermann, B., Kerick, M., Roehr, C., Fischer, A., Isau, M., Boerno, S. T., Wunderlich, A., Barmeyer, C., Seemann, P., Koenig, J., Lappe, M., Kuss, A. W., Garshasbi, M., Bertram, L., Trappe, K., Werber, M., Herrmann, B. G., Zatloukal, K., Lehrach, H., and Schweiger, M. R. (2010) Somatic mutation profiles of MSI and MSS colorectal cancer identified by whole exome next generation sequencing and bioinformatics analysis. *PLoS One* **5,** e15661
35. Field, S. J., Tsai, F. Y., Kuo, F., Zubiaga, A. M., Kaelin, W. G., Jr., Livingston, D. M., Orkin, S. H., and Greenberg, M. E. (1996) E2F-1 functions in mice to promote apoptosis and suppress proliferation. *Cell* **85,** 549–561
36. Ignáth, I., Hegyi, P., Venglovecz, V., Székely, C. A., Carr, G., Hasegawa, M., Inoue, M., Takács, T., Argent, B. E., Gray, M. A., and Rakonczay, Z., Jr. (2009) CFTR expression but not Cl- transport is involved in the stimulatory effect of bile acids on apical Cl-/HCO3- exchange activity in human pancreatic duct cells. *Pancreas* **38,** 921–929
37. Couzin, J. (2009) Biomarkers. Metabolite in urine may point to high-risk prostate cancer. *Science* **323,** 865
38. Bourgo, R. J., Ehmer, U., Sage, J., and Knudsen, E. S. (2011) RB deletion disrupts coordination between DNA replication licensing and mitotic entry in vivo. *Mol. Biol. Cell* **22,** 931–939
39. Pan, Q., Shai, O., Lee, L. J., Frey, B. J., and Blencowe, B. J. (2008) Deep surveying of alternative splicing complexity in the human transcriptome by high-throughput sequencing. *Nat. Genet.* **40,** 1413–1415
40. Orban, T. I., and Olah, E. (2003) Emerging roles of BRCA1 alternative splicing. *Mol. Pathol.* **56,** 191–197
41. Barbour, A. P., Reeder, J. A., Walsh, M. D., Fawcett, J., Antalis, T. M., and Gotley, D. C. (2003) Expression of the CD44v2–10 isoform confers a metastatic phenotype. Importance of the heparan sulfate attachment site CD44v3. *Cancer Res.* **63,** 887–892
42. Ward, A. J., and Cooper, T. A. (2010) The pathobiology of splicing. *J. Pathol.* **220,** 152–163
43. Piekielko-Witkowska, A., Wiszomirska, H., Wojcicka, A., Poplawski, P., Boguslawska, J., Tanski, Z., and Nauman, A. (2010) Disturbed expression of splicing factors in renal cancer affects alternative splicing of apoptosis regulators, oncogenes, and tumor suppressors. *PLoS One* **5,** e13690
44. Schmitt, C. A., Rosenthal, C. T., and Lowe, S. W. (2000) Genetic analysis of chemoresistance in primary murine lymphomas. *Nat. Med.* **6,** 1029–1035
45. Yoo, B. K., Gredler, R., Vozhilla, N., Su, Z. Z., Chen, D., Forcier, T., Shah, K., Saxena, U., Hansen, U., Fisher, P. B., and Sarkar, D. (2009) Identification of genes conferring resistance to 5-fluorouracil. *Proc. Natl. Acad. Sci. U.S.A.* **106,** 12938–12943
46. Noda, T., Nagano, H., Takemasa, I., Yoshioka, S., Murakami, M., Wada, H., Kobayashi, S., Marubashi, S., Takeda, Y., Dono, K., Umeshita, K., Matsuura, N., Matsubara, K., Doki, Y., Mori, M., and Monden, M. (2009) Activation of Wnt/β-catenin signalling pathway induces chemoresistance to interferon-α/5-fluorouracil combination therapy for hepatocellular carcinoma. *Br. J. Cancer* **100,** 1647–1658
47. Sharma, A., Upadhyay, A. K., and Bhat, M. K. (2009) Inhibition of Hsp27 and Hsp40 potentiates 5-fluorouracil and carboplatin mediated cell killing in hepatoma cells. *Cancer Biol. Ther.* **8,** 2106–2113